An analytical and numerical study of some aspects of the wood chipping process

Lisbeth M. Hellström, **Per Isaksson** and **Per A. Gradin**, Mid Sweden University, Sundsvall, **Kjell Eriksson**, Luleå University of Technology, Sweden

KEYWORDS: Wood chipping, Chip formation, Analytical model, Friction

SUMMARY: In order to model the wood chipping process, the primary process parameters have been identified and their first order interaction studied. The model is analytical and incorporates, in particular, the influence of sliding friction between the wood chipping tool and the log. To estimate the accuracy of the analytical model, a Finite Element (FE) analysis of the problem considered was also performed. The analytical model and the FE analysis are both restricted to small deformations and linear elastic orthotropic material behaviour. The most severe limitation with both the analytical and the FE model is the assumption of linearly elastic material. On the other hand, it is felt that existing models of anisotropic plasticity in metals are lacking too much of physical relevance, if applied to wood.

The analytical model predicts the normal and shear strain distribution in the crack-plane prior to crack initiation. The analytical distributions are in reasonable agreement with the corresponding distribution of the FE analysis.

Based on experimental findings, it is suggested that the stress field over the entire crack-plane, in conjunction with the stress field close to the tip of the chipping tool, are critical for chip creation, rather than just the latter.

ADDRESSES OF THE AUTHORS: Lisbeth M. Hellström (lisbeth.hellstrom@miun.se), **Per Isaksson** (per.isaksson@miun.se) and **Per A. Gradin** (per.gradin@miun.se): Mid Sweden University, Fibre Science and Communication Network, FSCN, Department of Natural Science, Engineering and Mathematics, SE-851 70 Sundsvall, Sweden. **Kjell Eriksson** (kjell.eriksson@ltu.se): Luleå University of Technology, SE-971 87 Luleå, Sweden.
Corresponding author: Lisbeth M. Hellström

A common demand in the pulp and paper industry today is the smallest possible variation of certain chip population parameters, in particular the chip thickness distribution. A narrow distribution promotes uniform product properties, e.g. in chemical impregnation processes, and is generally recognized as a characteristic of a high-quality product by consumers.

This means in practice that it is more important to produce chips of constant thickness rather than of a specific thickness and, in turn, that the chipping tool retains its characteristics over a long time rather than a pronounced sharpness. In order to predict the influence of, for example, tool wear on chip thickness, it is necessary to understand the underlying mechanisms of chip formation in detail.

In a previous investigation (Hellström et al. 2008) it was observed that the friction between the chipping tool and the wood greatly influenced the wood chipping process. Due to the inhomogeneous structure of wood, the friction coefficient varies over the cross section of a log and this might contribute to chip thickness scatter. To investigate further (at least in a qualitative way) the influence of pertinent parameters on the stress and strain fields in the chip, a simple analytical model was developed, assuming small deformations and a linear elastic orthotropic material. The model predicts the normal and shear strain distribution in the crack-plane prior to crack initiation and also the compressive force distribution on the chip-end. In order to roughly check the accuracy of the analytical model, a Finite Element (FE) analysis was also performed and the results of the two models were compared. It can be argued that more accurate results should be obtained with the FE analysis, but the analytical model, in conjunction, is transparent and offers a direct description of the relation between different parameters.

It was also found (Hellström et al. 2008) that just prior to the chip formation, there is a concentration of strains starting from the edge of the tool and extending along the grain direction, and further that the chipping tool indention process is approximately self-similar.

In addition, the (in an average sense) constant length-to-thickness ratio for a chip that has been experimentally observed and reported in the literature (c.f. Uhmeier 1995; Kivimaa, Murto 1949; Twaddle 1997; Hartler 1986) is also discussed.

Analytical study

To obtain at least qualitative results regarding the influence of different parameters and in particular of friction, a simple analytical model is considered. The model assumes sliding friction between chip tool and the log and is based on an assumed displacement field. The solution method exploits the theorem of minimum potential energy.

Material model

For the analytical model small deformations, a plane strain deformation and a linear elastic orthotropic material are assumed.

Elastic data (*see Table 1*) for wet spruce are taken from Uhmeier, Persson (1997):

Table 1 Material properties (Uhmeier and Persson, 1997)

E_L [MPa]	E_R [MPa]	G_{LR} [MPa]	ν_{LR}	ν_{RL}
10000	820	660	0.4	0.033

where *E, G* and ν are the Young's modulus, the shear modulus and the Poisson's ratio respectively. The subscripts *L, R* denote the principal material directions, namely the longitudinal and radial directions relative to the original log. The *L*, *R* directions correspond to the Cartesian *x*- and *y*- directions, respectively, of the model (see *Fig 1*)

Analytical model

Fig 1 shows a single wood chip, assumed to be clamped at the lower horizontal boundary. The cutting plane is at an angle β to the horizontal plane and the knife tip is occupying an angle α. The length and thickness of the chip are L and t, respectively. The coordinate system is such that the x-direction is parallel to the wood fibres and the y-direction perpendicular to the fibres.

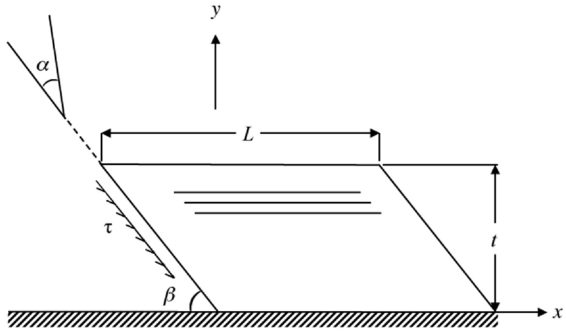

Fig 1. An idealised situation.

On the left boundary, a shear stress τ (for the time being left unspecified) is assumed to be acting. To simplify matters, coordinates ξ and η are used, and from *Fig 2* the coordinate transformation:

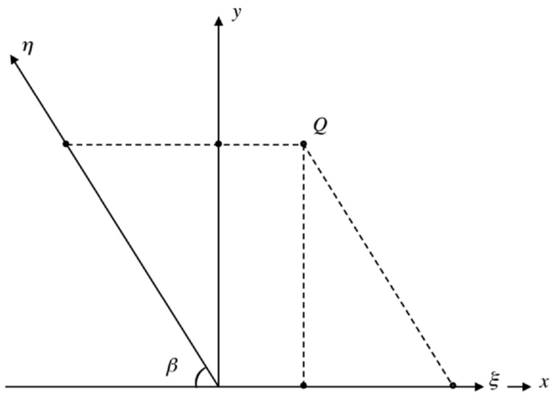

Fig 2. Coordinate transformation.

$$x = \xi - \eta \cos\beta \qquad [1]$$
$$y = \eta \sin\beta$$

is obtained.

In the following, derivatives with respect to x and y are obtained from *Eq 1*. For some arbitrary function $f(\xi, \eta)$ it follows that:

$$\frac{\partial f}{\partial x} = \frac{\partial f}{\partial \xi} \ and \ \frac{\partial f}{\partial y} = \frac{\left(\cos\beta\, \partial f / \partial\xi + \partial f / \partial\eta\right)}{\sin\beta} \qquad [2]$$

The boundary conditions to be satisfied are a) vanishing displacements u_x, u_y in the x- and y- directions respectively on the boundary $\eta = 0$, i.e. u_x and u_y equals zero on this boundary and b) a point on the cutting plane $\xi = 0$ is confined to move along a plane making the angle $\alpha + \beta$ with the x-axis.

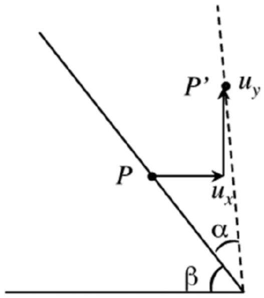

Fig 3. Sliding condition.

From *Fig 3* it is directly obtained that:

$$\tan\left(\alpha + \beta\right) = \frac{\eta \sin\beta + u_y\left(0, \eta\right)}{\eta \cos\beta - u_x\left(0, \eta\right)} \qquad [3]$$

α is assumed a small angle, consistent with the assumption of small deformations. Series expansion of the function $tan(\alpha + \beta)$ around β and ignoring higher order terms turns *Eq 3* into:

$$u_y\left(0, \eta\right) = \left(\alpha\eta - \sin\beta u_x\left(0, \eta\right)\right) / \cos\beta \qquad [4]$$

Assuming for $u_x(\xi, \eta)$ and $u_y(\xi, \eta)$ that:

$$u_x\left(\xi, \eta\right) = \eta f\left(\xi\right) \ and \ u_y\left(\xi, \eta\right) = \eta g\left(\xi\right) \qquad [5]$$

where f and g are functions to be determined, then one will have together with *Eq 4* that:

$$g\left(0\right) = \left(\alpha - \sin\beta f\left(0\right)\right) / \cos\beta \qquad [6]$$

The normal strains ε_x, ε_y and the shear strain γ_{xy} are found from the definitions of linear strains together with *Eq 2*:

$$\varepsilon_x = \eta f' \ and \ \varepsilon_y = (c\eta g' + g) / s \ and \ \gamma_{xy} = (c\eta f' + f) / s + \eta g' \qquad [7]$$

where a prime denotes differentiation with respect to ξ and $c = \cos\beta$ and $s = \sin\beta$ has been introduced for brevity. Note that the displacements given in *Eq 5* satisfies the requirement that the boundary $\eta = 0$ is clamped.

Since the only external load is the shear stress $\tau(\eta)$ on the boundary $\xi = 0$, the potential energy U is given by:

$$U = \int_S \frac{1}{2}\left(\sigma_x \varepsilon_x + \sigma_y \varepsilon_y + \tau_{xy}\gamma_{xy}\right) dS - \int_\Gamma \tau\left(cu_x - su_y\right) d\Gamma \qquad [8]$$

where σ_x, σ_y and τ_{xy} are the normal and shear stresses, respectively, S is the domain in the (x-y) plane, occupied by the chip and Γ denotes the boundary $\xi = 0$. An orthotropic linear elastic material, is defined by the following relation:

$$\begin{bmatrix} \sigma_x \\ \sigma_y \\ \tau_{xy} \end{bmatrix} = \begin{bmatrix} C_{11} & C_{12} & 0 \\ C_{12} & C_{22} & 0 \\ 0 & 0 & C_{66} \end{bmatrix} \begin{bmatrix} \varepsilon_x \\ \varepsilon_y \\ \gamma_{xy} \end{bmatrix} \qquad [9]$$

where C_{11}, C_{12} … C_{66} are elastic constants. Substitution of *Eq 9* into *Eq 8* yields:

$$U = \int_S \frac{1}{2}(C_{11}\varepsilon_x^2 + 2C_{12}\varepsilon_x\varepsilon_y + C_{22}\varepsilon_y^2 + C_{66}\gamma_{xy}^2)dS - \int_\Gamma \tau(cu_x - su_y)d\Gamma \quad [10]$$

The variation of U with respect to the strains, result in:

$$\delta U = \int_S (C_{11}\varepsilon_x\delta\varepsilon_x + C_{12}(\varepsilon_x\delta\varepsilon_x + \varepsilon_y\delta\varepsilon_y) + C_{22}\varepsilon_y\delta\varepsilon_y + C_{66}\gamma_{xy}\delta\gamma_{xy})dS - \int_\Gamma \tau(c\delta u_x - s\delta u_y)d\Gamma \quad [11]$$

Now, substitution of the strains given by *Eq 7* into *Eq 11* gives an expression involving the functions f, f', g, g' and their variations. Performing integration by parts on all terms involving $\delta f'$ and $\delta g'$ with respect to ξ and further integration with respect to η results in:

$$\begin{aligned}\delta U = s\int_0^L &((-I_1 f'' - I_2 g'' + I_3 g' + I_4 f)\delta f \\ &+ (-I_5 g'' - I_2 f'' - I_3 f' + I_6 g)\delta g)d\xi \\ &+ s\left[(I_1 f' + J_1 f + I_2 g' + J_2 g)\delta f\right]_0^L \\ &+ s\left[(I_2 f' + J_3 f + I_5 g' + J_4 g)\delta g\right]_0^L \\ &- \int_\Gamma \tau\left(c\delta u_x - s\delta u_y\right)d\Gamma = 0\end{aligned} \quad [12]$$

where I_1, I_2... and J_1, J_2... are defined in **Appendix**. For *Eq 12* to hold for arbitrary variations δf and δg in the open interval $0 < \xi < L$, the following must hold:

$$I_1 f'' + I_2 g'' - I_3 g' - I_4 f = 0 \quad [13]$$

$$I_5 g'' + I_2 f'' + I_3 f' - I_6 g = 0 \quad [14]$$

Also, at $\xi = L$:

$$I_1 f' + J_1 f + I_2 g' + J_2 g = 0 \quad [15]$$

$$I_2 f' + J_3 f + I_5 g' + J_4 g = 0 \quad [16]$$

Now it is timely to specify $\tau(\eta)$. Since the ambition is to include sliding friction in a consistent way and since it is a simple matter to show that the stresses and hence the contact pressure will be linear in η, it is assumed for $\tau(\eta)$:

$$\tau(\eta) = k_\tau\eta + m_\tau \quad [17]$$

where k_τ and m_τ are constants to be determined. With $\tau(\eta)$ given by *Eq 17* the line integral in *Eq 12* will become:

$$-\int_\Gamma \tau\left(c\delta u_x - s\delta u_y\right)d\Gamma = K_1\delta g(0) - K_2\delta f(0) \quad [18]$$

K_1 and K_2 both depend linearly on k_τ and m_τ and are given in **Appendix**. When $\xi = 0$, δf and δg are not independent but subjected to *Eq 6* so that at $\xi = 0$ (note again, that for brevity $s = \sin\beta$ and $c = \cos\beta$):

$$I_1 f' + J_1 f + I_2 g' + J_2 g - \left(I_2 f' + J_3 f + I_5 g' + J_4 g\right)s/c = -K_2/s + K_1/c \quad [19]$$

In addition, *Eq 6* has to be satisfied i.e.:

$$g(0) = \left(\alpha - sf(0)\right)/c \quad [6']$$

The solution to *Eqs 13* and *14* can easily be shown to be:

$$f(\xi) = A\cosh(\lambda_1\xi) + B\sinh(\lambda_1\xi) + C\cosh(\lambda_2\xi) + D\sinh(\lambda_2\xi) \quad [20]$$

$$g(\xi) = A\gamma_1\cosh(\lambda_1\xi) + B\gamma_1\sinh(\lambda_1\xi) + C\gamma_2\cosh(\lambda_2\xi) + D\gamma_2\sinh(\lambda_2\xi) \quad [21]$$

where A to D are constants, determined through the conditions in *Eqs 6, 15, 16* and *19* and λ_1, λ_2, γ_1 and γ_2 are defined in **Appendix**.

Having obtained f and g, these are substituted into *Eq 7* to obtain the strains, which together with *Eq 9* will give the stresses and in particular, the contact pressure p on the boundary $\xi = 0$ is given in terms of the stresses on this boundary by:

$$p = -\left(\sigma_y c^2 + \sigma_x s^2 + 2\tau_{xy}cs\right) \quad [22]$$

Now, since Coulomb sliding friction is assumed one will have:

$$\tau = \mu p \quad [23]$$

where $\mu \geq 0$ is the coefficient of friction.

Because linear conditions are assumed, the contact pressure must depend linearly on the loading parameters, i.e. on α, so that (remembering that p is linear in η):

$$p = \left(a_\alpha\alpha + a_k k_\tau + a_m m_\tau\right)\eta + b_\alpha\alpha + b_\tau k_\tau + b_m m_\tau \quad [24]$$

where a_α, a_k ….. b_m are influence coefficients. These can easily be determined by assigning nonzero values to one of α, k_τ and m_τ, while keeping the others equal to zero. It should be pointed out that $k_\tau = m_\tau = 0$ i.e. $\tau = 0$ is consistent with $\mu = 0$ in *Eq 23*. No closed form expressions for these coefficients are derived but they are determined numerically. Now, to get, for a given value of α, a consistent model for sliding friction, one must have with *Eq 17* and *Eq 24* that:

$$k_\tau\eta + m_\tau = \mu\left[\left(a_\alpha\alpha + a_k k_\tau + a_m m_\tau\right)\eta + b_\alpha\alpha + b_k k_\tau + b_m m_\tau\right] \quad [25]$$

This will give two equations, from which k_τ and m_τ can be determined, and having done so, K_1 and K_2 can be calculated and inserted into *Eq 19* and an approximate solution for a case of sliding friction is obtained.

FE- model

In order to estimate the accuracy of the analytical model, a FE analysis was also performed.

The problem considered was analyzed by using a 2D finite element code, implemented in the Matlab (2007) software, with conventional four-node iso-parametric elements of two degrees of freedom, translation in the x- and y-directions. A full description of the element properties and the implementation procedure can be found in Bathe (1982).

An iterative technique has been employed to solve the equilibrium equations. The crack surfaces contact algorithm employed uses constraint functions to enforce all contact conditions of the Coulomb-friction contact at the contact nodes (cf. Adina, 1995). The result obtained after each iteration then corresponds to estimates of the incremental displacements from which the current stress is computed. All deformations are assumed small so that linear relations for equilibrium and kinematics are applicable and all derivatives and integrals are evaluated with respect to the initial topology of the considered geometry.

Results

With elastic data taken from *Table 1*, the stresses σ_y and τ_{xy} are calculated along the crack-plane for $\alpha = 10°$, $L = 25$ mm, $t = 5$ mm, $\mu = 0{,}2$ and $\beta = 60°$ and $\beta = 70°$ for both models and are shown versus ξ/t and normalized with respect to E_R in *Figs 4* and *5*.

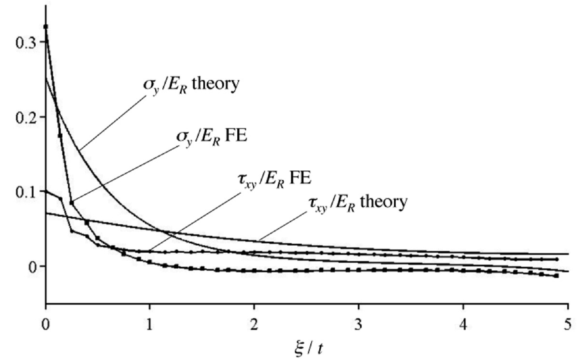

Fig 4. Normalized stresses σ_y/E_R and τ_{xy}/E_R along the crack-plane for the case $\beta = 60°$ and $\mu = 0{,}2$.

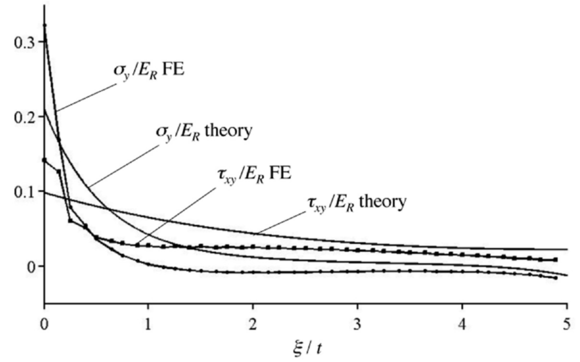

Fig 5. Normalized stresses σ_y/E_R and τ_{xy}/E_R along the crack-plane for the case $\beta = 70°$ and $\mu = 0{,}2$.

Comparison of results

Selected results of the analytical model were compared to the corresponding results of the FE analysis (*Figs 4 and 5*). The analytical stresses σ_y and τ_{xy} along the crack-plane agree reasonably well with the FE stresses. The agreements of the shape of the curves are relatively good, but the magnitudes differ more in the region close to the chipping tool. Further, the agreement is better for stresses calculated for larger values of β. For smaller values of β, the assumption made regarding the displacement becomes insufficient.

Discussion

It has been reported in the literature (c.f. Uhmeier 1995; Kivimaa, Murto 1949; Twaddle 1997; Hartler 1986) that for the same process parameters and geometry of the chipping tool, the ratio between length and thickness of the chip is (in some average sense) constant. Some consequences of this observation will now be discussed. Consider *Fig 6* below:

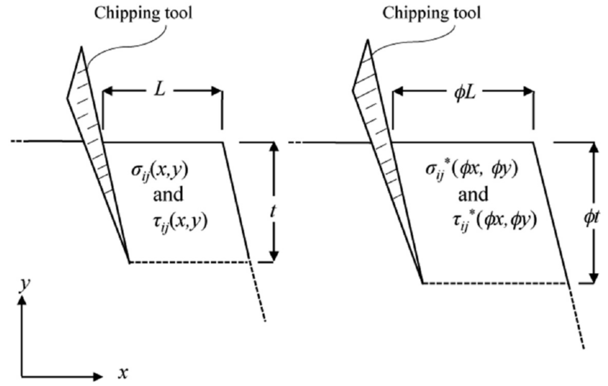

Fig 6. Quarter infinite geometries.

If it is assumed that there are no intrinsic length scales associated with the material, then the stress and strain fields in the left geometry i.e. $\sigma_{ij}(x, y)$ and $\varepsilon_{ij}(x, y)$ will be related to the same fields in the scaled geometry according to:

$$\sigma_{ij}\left(x,y\right)=\sigma_{ij}^{*}\left(\phi x,\phi y\right) \text{ and } \varepsilon_{ij}\left(x,y\right)=\varepsilon_{ij}^{*}\left(\phi x,\phi y\right) \quad [26]$$

This is often referred to as self-similarity. Obviously, the assumption that there are no intrinsic length scales associated with wood, is not true since wood does indeed possess a structure. On a macroscopic length scale an annual ring structure can be identified and on a smaller length scale, a fibre structure can be seen etc. However, in spite of this, it is shown in Hellström et al. (2008), in agreement with the previous reports, that the wood chipping process is approximately (at least for the cases considered) self-similar.

Assuming that self-similarity holds, then the stresses along the horizontal plane indicated in *Fig 6*, will be identical in the normalised x- coordinate $\psi = x/(\phi L)$, for all values of ϕ. In the same way, the stresses along the left inclined plane will be the same in the normalised coordinates $\upsilon = y/(\phi t)$.

Let F be the cutting force, i.e., the force in the direction of the chipping tool. For a tool with a knife angle $\alpha > 0$ the force F initially increases with the depth of penetration of the tool, because of the wedging action. The horizontal component of F, here denoted F_H, is carried by the wood piece ligament, i.e., the remaining, uncut cross section of the wood piece, ahead of and in the plane of the cutting tool. The load carrying capacity of the ligament decreases however with the depth of penetration.

The two extreme points above taken together imply that the cutting force attains a maximum at some critical depth of penetration, depending on the relation between the tool contact stress and strength of the ligament.

It has been observed in the experiments that short cracks, with a fairly regular distribution, are formed along the cut surfaces as the chipping tool penetrates a wood piece. The length of the cracks does, however, not increase with depth of penetration. A further observation is that a chip is formed at a critical relative, not absolute, penetration depth.

Now, if the intensity of the stress state at the tip of the cutting tool increases with the depth of penetration and chip formation is governed solely by a local criterion, then a chip would always form at an absolute tool penetration depth, which means that the chip thickness would be constant, or nearly so. In view of reported results and the experimental observations, it thus seems unlikely that chip formation is governed by a local criterion only.

The horizontal force F_H is related to the cutting force and thereby to the depth of penetration, it being proportional to the depth of penetration, or very nearly so.

For example, a uniformly expanding friction free and flat elliptical tool in a very wide plate is accompanied by a constant contact normal stress perpendicular to the major axis of the ellipse, i.e. the length of the tool. As the contact stress is constant along the tool, the corresponding resultant force is exactly proportional to the tool length.

It is reasonable to assume that to any given cutting geometry there exists a corresponding ideal tool shape for which the horizontal force is exactly proportional to the depth of penetration. A wedge with straight sides, as in the present case, is not likely of ideal shape and therefore no stronger assumption than the horizontal force be only nearly proportional to the penetration depth, seems justified.

Now, wood is a highly non-isotropic material and a crack propagates much more easily along the fibres than in other directions. Consider, therefore, the prospective horizontal crack plane passing through the tip of the chipping tool. From equilibrium, the resultant force on this plane amounts to F_H.

Recall that, at least initially, F_H increases with penetration depth. It is reasonable to assume that failure along this plane occurs as F_H attains a critical value, whether failure occurs through crack extension from the tool tip and onwards or through a global mechanism of instability involving the entire crack plane.

Further, it is assumed that the critical value for failure is related to the length of the crack plane. Derivation of an accurate relationship requires a detailed study, but the very simple assumption that that the critical value just increases with the length of the crack plane seems justified and is sufficient at present.

Thus the stress state at the tip of the tool, in conjunction with the stress field over the entire crack plane, is critical for chip formation, rather than the former stress field solely. As the horizontal force F_H increases with penetration depth and the corresponding critical value with crack plane length, it follows that the chip thickness to length ratio is constant, or that the two-criteria condition for chip formation is consistent with self-similarity.

This situation is very much unlike what is seen in e.g. fracture mechanics where the crack length has critical influence on strength. Another example is the strength of an infinite plate with a circular hole, of a composite material, where the diameter of the hole influences the strength.

Conclusions

To start with, it must be mentioned when performing the calculations involving both the analytical and the FE-model the fact that β has an influence on the thickness was ignored i.e. the same chip thickness was assumed for different β:s.

The analytical model indicates a large influence of β on the magnitude of τ_{xy} i.e. a small value of β will give a more pronounced opening mode compared to a large value of β. The model also predicts a decreasing contact pressure with a decreasing β.

It was also observed that the model indicated contact stresses being tensile in a region close to the tip of the chipping tool. This is due to that the assumed displacements in *Eq 5* are too simple. However and in spite of this, the model predicts a decreasing contact pressure with a decreasing β.

Due to lack of experimental data, the stresses could not be verified experimentally.

However, the analytical model predicts the normal and shear stress distribution in the crack-plane, which is in reasonable agreement the FE analysis.

Finally it is concluded that it is not only the stress field close to the tip of the tool that determines the creation of a chip, but it is the stress field over the entire crack-plane that is critical.

Acknowledgements

The Swedish KK-Foundation and the European Regional Development Fund are acknowledged for financial support.

Literature

ADINA R&D Inc. (1995): Theory and Modelling Guide, Watertown MA, USA.

Bathe, K.J. (1982): Finite element procedure in engineering analysis, Prentice-Hall, USA.

Hartler, N. (1986): Chipper design and operation for optimum chip quality, Tappi J. 69(10), 62.

Hellström, L.M., Gradin, P.A. and Carlberg, T. (2008): A method for experimental investigation of the wood chipping process, Nord. Pulp Paper Res. J. 23(3), 339.

Kivimaa, E. and Murto, J.O. (1949): Investigations on factors affecting chipping of pulp wood, Statens Tekniska Forskningsanstalt (VTT), Finland Publ. 9.

Matlab (2007): Version 7.4. The MathWorks Inc., Natick, MA, USA.

Twaddle, A. (1997): The influence of species, chip length, and ring orientation on chip thickness, Tappi J. 80(6) 123.

Uhmeier, A. (1995): Some fundamental aspects of wood chipping, Tappi J. 78(10), 79.

Uhmeier, A. and Persson, K. (1997): Numerical Analysis of Wood Chipping, Holzforschung, 51(1), 83.

Manuscript received October 15, 2008
Accepted February 23, 2009

Appendix ▶

Appendix

$s = \sin\beta$ and $c = \cos\beta$

$$\eta_t = \frac{t}{\sin\beta}$$

$$I_1 = \left(C_{11} + C_{66}\frac{c^2}{s^2} \right)\frac{\eta_t^3}{3}$$

$$I_2 = \left(C_{12} + C_{66} \right)\frac{c}{s}\frac{\eta_t^3}{3}$$

$$I_3 = -\left(C_{12} - C_{66} \right)\frac{\eta_t^2}{2s}$$

$$I_4 = \frac{C_{66}}{s^2}\eta_t$$

$$I_5 = \left(C_{22}\frac{c^2}{s^2} + C_{66} \right)\frac{\eta_t^3}{3}$$

$$I_6 = \frac{C_{22}}{s^2}\eta_t$$

$$J_1 = C_{66}\frac{c}{s^2}\frac{\eta_t^2}{2}$$

$$J_2 = \frac{C_{12}}{s}\frac{\eta_t^2}{2}$$

$$J_3 = \frac{C_{66}}{s}\frac{\eta_t^2}{2}$$

$$J_4 = C_{22}\frac{c}{s^2}\frac{\eta_t^2}{2}$$

$$K_1 = s\left(\frac{k_\tau \eta_t^3}{3} + \frac{m_\tau \eta_t^2}{2} \right)$$

$$K_2 = c\left(\frac{k_\tau \eta_t^3}{3} + \frac{m_\tau \eta_t^2}{2} \right)$$

$$\lambda_A = \frac{I_1 I_6 + I_4 I_5 - I_3^2}{2\left(I_1 I_5 - I_2^2 \right)} + \sqrt{\frac{1}{4}\left(\frac{I_1 I_6 + I_4 I_5 - I_3^2}{I_1 I_5 - I_2^2} \right)^2 - \frac{I_4 I_6}{I_1 I_5 - I_2^2}}$$

$$\lambda_B = \frac{I_1 I_6 + I_4 I_5 - I_3^2}{2\left(I_1 I_5 - I_2^2 \right)} - \sqrt{\frac{1}{4}\left(\frac{I_1 I_6 + I_4 I_5 - I_3^2}{I_1 I_5 - I_2^2} \right)^2 - \frac{I_4 I_6}{I_1 I_5 - I_2^2}}$$

$$\lambda_1 = \sqrt{\lambda_A}$$

$$\lambda_2 = \sqrt{\lambda_B}$$

$$\gamma_1 = -\frac{\left(I_1 \lambda_1^2 - I_4 \right)}{\lambda_1 \left(I_2 \lambda_1 - I_3 \right)}$$

$$\gamma_2 = -\frac{\left(I_1 \lambda_2^2 - I_4 \right)}{\lambda_2 \left(I_2 \lambda_2 - I_3 \right)}$$